Orientational Instability of Vicinal Pt Surfaces Close to (111)

Elmar Hahn, Hansjörg Schief, Vittorio Marsico, Alexander Fricke, and Klaus Kern
Institut de Physique Expérimentale, École Polytechnique Fédérale de Lausanne, CH-1015 Lausanne, Switzerland
(Received 10 November 1993)

Using scanning tunneling microscopy and thermal He diffraction we have studied the morphology of the vicinal Pt(997) surface, close to the hexagonal close-packed (111) face. While oxygen adsorption induces a step-doubling transition, the clean surface is thermally unstable towards faceting. Above $T \approx 0.5T_m$ the surface is found to undergo partial phase separation into large {111} facets and regions of undisturbed step regions. The faceted phase is stabilized by a reduction of surface stress through reconstruction of the (111) faces. The faceting is found to proceed via a nucleation-and-growth mechanism.

PACS numbers: 68.35.Rh, 61.16.Ch, 68.35.Bs, 82.65.Dp

The structure of vicinal surfaces, i.e., regularly stepped surfaces which are generated by a slight miscut with respect to a low-index plane, has been the subject of many recent studies [1–4]. They constitute ideal model systems to study the relation between surface structure and surface energy. Nominally, vicinal surfaces are composed of terraces of the low-index orientation separated by a superlattice of parallel steps accommodating the misorientation θ. The total surface energy $\gamma(\theta,T)$ of the vicinal is given by

$$\gamma(\theta,T) = \gamma_0(T) + [\beta(T)/h]|\tan\theta| + [B(T)/a_{\parallel}h^3]|\tan\theta|^3 . \quad (1)$$

The first term γ_0 is the surface energy of the low-index terraces while the second term adds the contribution from each of the monatomic steps, with β being the energy per unit length to form an isolated monatomic step of height h. The last term B accounts for interactions between neighboring steps and $a_{\parallel}$ is the unit vector along the step edge. The nominal structure is only stable if the vicinal orientation is a tangent in the Wulff plot (γ versus θ) in polar form [5]. Unstable orientations phase separate into a "hill and valley structure" of coexisting regions of stable low-index orientations (facets).

Because of the delicate balance between step and terrace energies also stable vicinals can be subject to morphological changes as a function of temperature or impurity concentration. The ordered superlattice of equally spaced steps is stabilized by the repulsive step-step interaction between neighboring steps. At elevated temperatures thermal disorder through excitation of kinks competes with the order established by the repulsive step-step interaction. This thermal kink proliferation eventually results in a roughening transition of the vicinal surface [6]. Changes in temperature might also modify the terrace and step-free energies, and thereby induce an orientational instability. So far only three examples of thermal faceting of clean surfaces are known: vicinal Si surfaces close to (111) and vicinal Pt surfaces close to (100) where the orientational instability is induced by reconstruction [2,7] and vicinal Pb surfaces close to (111) where faceting is driven by surface melting [8]. More frequently observed are faceting transitions induced by impurity adsorption [9].

In this Letter we report measurements of temperature and impurity induced changes in the surface morphology of the vicinal Pt(997) surface. Nominally this vicinal surface is composed of close-packed (111) terraces separated each 20.2 Å by a monatomic step with {111} microfacet [Fig. 1(a)]. Early measurements of Comsa, Mechtersheimer, and Poelsema indicated that oxygen adsorption can provoke step doubling or faceting (depend-

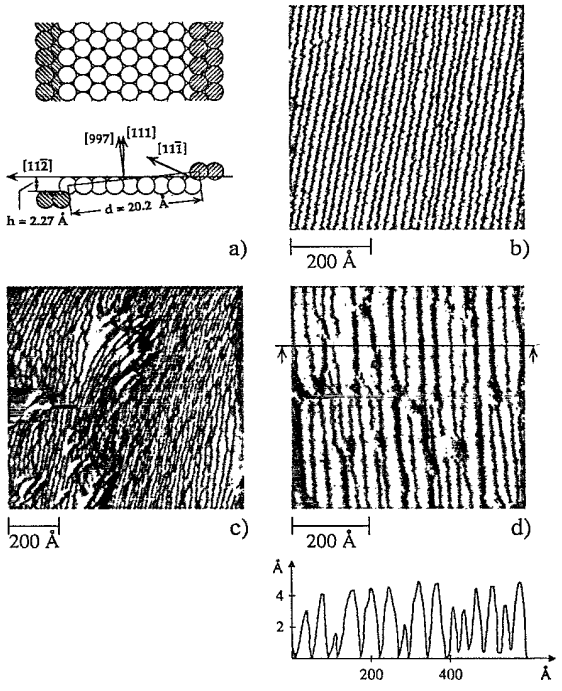

FIG. 1. The terrace-step ordering of Pt(997). (a) Schematic model of the nominal structure. (b) STM image of the clean and well ordered surface, annealed at 900 K and slowly cooled to 300 K. (c) STM image of the surface in the presence of small amounts of impurities. (d) STM image of the surface after annealing in an oxygen atmostphere of 1×10^{-7} mbar at 700 K; the surface partially shows step doubling. This is clearly evident in the height scan taken from the corresponding absolute STM topograph.

0031-9007/94/72(21)/3378(4)$06.00

ing on temperature) of this vicinal surface [10,11]. We will demonstrate here that the step-doubling transition is indeed caused by oxygen impurities while the faceting transition at $T \approx 0.5 T_m$ is a property of the clean surface, related to the inherent instability of (111) terraces towards reconstruction. The faceting is shown to proceed via a nucleation-and-growth mechanism.

The morphology changes of the Pt(997) surface have been studied by scanning tunneling microscopy (STM) and high-resolution He diffraction. The variable temperature STM (150–600 K) is a home-built modified "beetle" type microscope which is coupled to a cryogenic sample holder in ultrahigh vacuum [12]. The Pt(997) crystal was prepared and cleaned in the usual way [10,11]. Surface cleanliness was carefully checked by Auger spectroscopy. Because the morphology changes occur outside the accessible temperature range of the STM we have studied them with a quench technique. After careful equilibration at the desired surface temperature the sample is rapidly quenched to room temperature, in order to freeze in the obtained morphology. The efficiency of the freezing procedure has been demonstrated recently by Michely and Comsa for island and defect structures on Pt(111) [13]. The He-diffraction measurements have been performed with a novel He-triple-axis spectrometer using double-surface scattering; the basic principle of the diffractometer is described in Ref. [14].

Figure 1(b) displays a typical STM image of the Pt(997) surface which has been carefully prepared by sputtering and successive annealing at 900 K. The surface shows a terrace-step arrangement close to its nominal structure, with terrace widths varying moderately around their nominal width of 20.2 Å. Measurements of the step heights revealed that only monatomic steps are present at the surface. In the presence of small amounts of impurities the steps are pinned during the annealing and locally the terrace-step order is lost. An example of such a situation is shown in Fig. 1(c); here the sample was deliberately contaminated with a few percent of carbon.

In view of a more quantitative characterization of the clean, well ordered Pt(997) surface, we calculated the probability distribution for the distances between neighboring steps, analyzing 1000 individual line scans from twelve STM images; the result is shown in Fig. 2. The measured distribution is compared with the predictions of the terrace-step-kink model (TSK) [6,15] and a model of Williams and Bartelt (WB, solid line) [2,15]. The TSK model assumes no energetic interactions between the steps. However, the meandering of a step is limited by its inability to cross neighboring steps. This leads to a decrease in the entropy of meandering and to an effective entropic repulsion between steps. The terrace-width distribution function of this entropic model is asymmetric with a bias against small step separations. Our data are clearly not consistent with the TSK distribution: The Pt(997) surface exhibits a Gaussian distribution centered

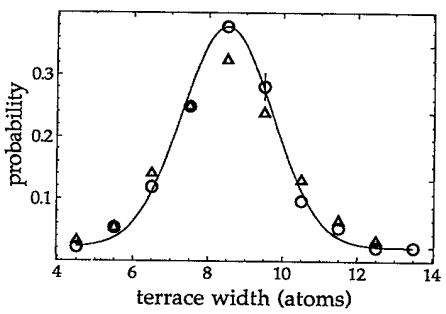

FIG. 2. Terrace width distribution of the Pt(997) surface after annealing at 900 K and slow cooling (○) and rapid quenching (△) to 300 K. The experimental data are compared with the model of Williams and Bartelt (full line); for details see text.

around the nominal width of 8.5 atom spacings. Such a distribution is consistent with the WB model indicating the presence of additional step-step interactions $U(x)$; here x is the coordinate perpendicular to the step edge. The WB model yields a symmetric terrace-width distribution, which can be approximated by the function $P(x,l) = (l/w\sqrt{(2\pi)}) \exp(-x^2/2w^2)$ [15]. The solid line in Fig. 2 shows the best fit with the width parameter $w = 2.9$ Å. For step-step interactions of the form $U(x) = A/x^2$ (elastic or dipole-induced interactions) the ratio w/l is a direct measure of the ratio of the step interaction strength A to the entropic interaction g. From our value $w/l = 0.14$ we determine $A/g = 59.6/a_{\|}$. Accordingly the magnitude of the step interaction term in the total free energy is increased by 2 orders of magnitude compared to the TSK model with entropically meandering steps only; i.e., $B(T) = 108 g(T)$. The strength of the elastic and/or dipole step-step interactions of the vicinal platinum surface is thus 1 order of magnitude larger than on vicinal silicon surfaces [2].

The Pt(997) surface is orientationally unstable to both impurity adsorption and temperature variations. The influence of oxygen adsorption on the morphology is shown in Fig. 1(d). In this STM image the surface has been annealed in an oxygen atmosphere (1×10^{-7} mbar) at 700 K for several minutes before quenching to room temperature. In the image we recognize step-doubled regions coexisting with small regions of the "nominal" single-step arrangement. The step-terrace ordering of the step-doubled regions is by far less regular than the order on the clean surface [Fig. 1(b)]. The phase separation between the step-doubled and the single-step regions in Fig. 1(d) appears to be stabilized by oxides which are imaged as bright bulbs, preventing a further growth of the double terraces.

The thermal evolution of the Pt(997) surface morphology is demonstrated in Figs. 2 and 3. Up to temperatures of 900 K the single-step vicinal arrangement is perfectly stable showing only a slight increase in the width of the step-distance distribution (see Fig. 2) with increasing temperature. Above 900 K the surface morphology, how-

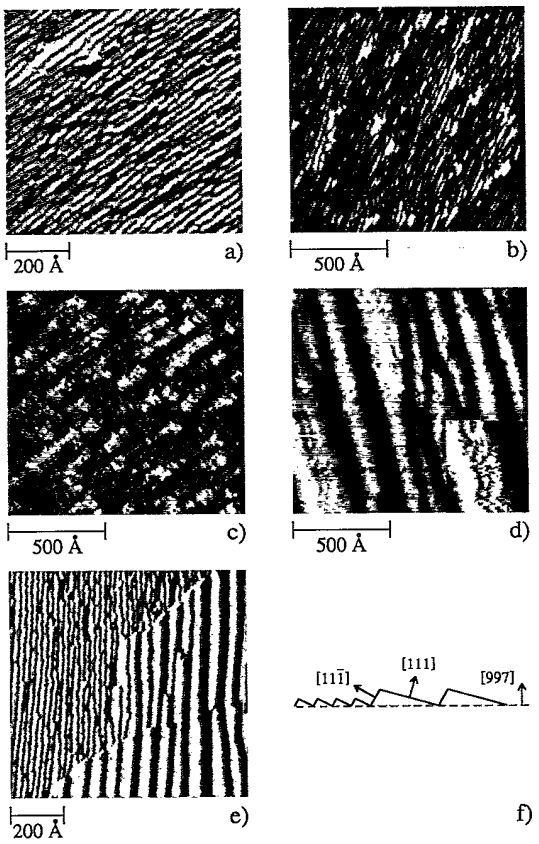

FIG. 3. Thermal faceting of the Pt(997) surface. The figure shows STM images of the quenched morphology (300 K) after annealing to (a) 920, (b) 980, (c) 1060, (d) 1160, and (e) 1150 K. In (f) we show a schematic model of the faceted surface.

ever, dramatically changes (see Fig. 3). At 920 K we observe a low density (about 4×10^{-7} Å^{-2}) of local distortions on the surface. At these distortions a few steps bunch together, generating extended flat (111) terraces of nearly double and triple width. In contrast to the case in Fig. 1(c) where the step pinning is caused by impurities (clearly visible in the STM images and in the Auger spectrum) we have no indication for the presence of impurities in Fig. 3(a); within the detection limit no sign of impurities has been seen in the corresponding Auger spectra. With increasing temperature the density and extension of the distortions increases. At 980 K [Fig. 3(b)] we measure a density of 2×10^{-5} Å^{-2} and the distorted (111) terraces are now already extending up to three or four nominal terrace widths; we see the beginning faceting of the surface. Increasing the temperature to 1060 K [Fig. 3(c)] the local (111) facets are growing further in size, while their density is nearly unchanged. At 1160 K [Fig. 3(d)] we finally have fully faceted regions on the surface. The series of STM images clearly reveals the nucleation-and-growth mechanism of the thermal faceting. With increasing temperature first the number of nucleation centers increases until a saturation density is reached. Upon further increase of the temperature the facet nuclei grow in size and finally large surface regions become faceted via coalescence. However, like in the step-doubling transitions, the restructured phase is always in coexistence with the nominal single-step phase, as demonstrated in Fig. 3(e). The image clearly reveals the presence of two coexisting regions on the surface: A completely faceted phase and a single-step phase with nominal structure. The nominal single-step region shows an almost perfect step ordering similar to the situation in Fig. 1(b). The phase boundary between faceted and nominal regions is very abrupt and seems not to be stabilized by impurities. The image reveals also a surprising detail of the faceted region; the individual facets appear to be ordered in a nearly periodic one-dimensional pattern. The thermal faceting of the Pt(997) surface appears to be reversible; annealing a partially faceted surfaced for several minutes at 900 K restores the nominal phase.

In the following we want to address the physical origin of the impurity and temperature induced morphological changes of the vicinal Pt(997) surface. The actual morphology of a vicinal surface is determined by the delicate balance between the step creation energy β, the step-step repulsion energy B, and the terrace energy γ_0. An initially stable vicinal surface will be subject to an orientational instability if a physical (temperature) or chemical (impurity) process affects selectively the energy costs of steps or the terrace energy or if the process affects both energies with different sign [16].

We first discuss the oxygen induced step doubling. Sibener and co-workers have recently observed such a transition on a vicinal Ni surface close to (111) [17]. In their He-scattering study they were able to determine the critical oxygen coverage which is necessary to induce step doubling. The critical oxygen coverage was found to be very close to the number density of Ni step sites, suggesting that step doubling might be caused by modification of the step energy. On the clean surface an isolated double step costs more energy than two isolated single steps. If the decoration of the steps with oxygen lowers the energy cost for the creation of double steps, this energy cost might be outweighted by the decrease in step repulsion energy since double steps increase the average step separation. As a net result the stable surface morphology will be a regular vicinal surface with double-height steps every 40.4 Å.

The thermal faceting, on the other hand, appears to be driven by a change in terrace energy. At low temperatures the Pt(111) terraces are known to bear a substantial tensile stress of about 0.35 eV Å^{-2} [18]. In a surface under tensile stress the atoms are sitting at lower density than is optimal and there is a tendency for contraction in the surface to increase the density towards the optimal value, thereby releasing the surface stress (i.e., lowering the surface energy γ_0). The Pt(111) surface has thus an inherent tendency to surface reconstruction through a

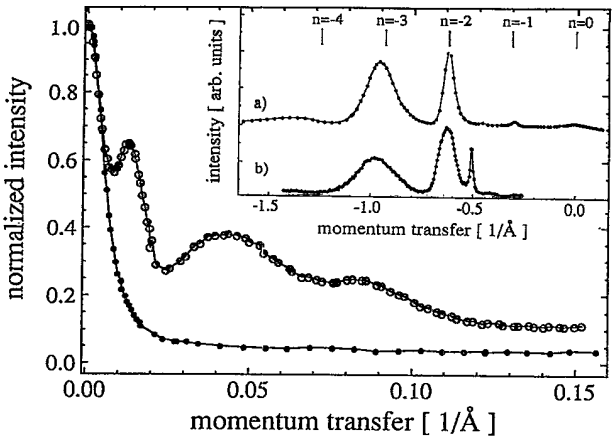

FIG. 4. High-resolution He-diffraction scans on Pt(997); see text. Open dots: close-up of the specular peak of the {111} facets taken with a primary beam wavelength of 0.535 Å and a specular diffraction condition $\vartheta_i = 69.35°$. Full dots: close-up of the three-dimensional diffraction peak of the nominal Pt(997) surface with the same primary wavelength and $\vartheta_i = 75.75°$. Inset: diffraction scans of the nominal surface (*a*) and the partially faceted surface (*b*) taken under identical scattering conditions ($\lambda = 0.96$ Å, $\vartheta_i = 76.0°$).

transfer of excess atoms into the surface layer. Recent experiments of Bott *et al.* [19] and Sandy *et al.* [20] demonstrate that such a reconstruction can indeed be induced on Pt(111) upon applying an enhanced Pt gas-phase chemical potential or by heating the surface to temperatures above about 1300 K. In the reconstructed phase the excess surface atoms are accommodated in a hexagonal domain wall network, characterized by a typical length of about 100–200 Å. We will demonstrate below that the thermal faceting of the Pt(997) surface is related to the temperature induced stress relief of the (111) terraces via reconstruction. The mesoscopic domain wall network of the reconstructed (111) surface with its characteristic length of more than 100 Å can only develop on sufficiently large terraces driving the Pt(997) faceting at elevated temperatures.

A first indication for the presence of a domain wall network on the (111) terraces of the facets is given in the inset of the STM image Fig. 3(d). The image reveals the presence of faint corrugation lines, which might be frozen domain walls. The decisive proof for the reconstruction is given by the He-diffraction measurements shown in Fig. 4, which have been obtained with the scattering plane oriented along the $[11\bar{2}]$ direction. In the inset of Fig. 4 we show two diffraction scans from the unfaceted surface (curve *a*) and the partially faceted surface (curve *b*). The faceted surface was prepared by extensive annealing at 1200 K and subsequent rapid quenching to 160 K. Whereas in the upper diffraction scan all peaks can be assigned to two-dimensional Bragg rods of the nominal Pt(997) surface, one additional sharp peak corresponding to the specular direction of the {111} facets appears in the scan of the faceted surface. Subsequently we have measured a precise He-diffraction profile around the specular peak of the {111} facets (open dots). The position of the facet specular in the close-up has been set to zero momentum transfer. Three diffraction signatures are clearly present: a relatively sharp peak at 0.013 $Å^{-1}$ and two broad peaks at 0.043 and 0.084 $Å^{-1}$. The sharp peak close to the specular position can be associated with the "mesoscopic" facet ordering. The two broad diffraction peaks (first and second order) at larger momentum transfers are signatures of the terrace reconstruction. The inferred real space distance of 146 Å nicely agrees with the characteristic distance of the domain wall network of 100–200 Å as inferred from x-ray diffraction measurements [20]. In Fig. 4 we also compare the facet-specular peak with a diffraction scan at the three-dimensional Bragg point of the unfaceted Pt(997) surface (full dots). The sharp profile clearly demonstrates the absence of any additional long-range order or crystal twinning on the nominal surface.

We finally want to point out that there is also a close similarity in the manifestation of the reconstruction of Pt(111) and the faceting of Pt(997). In both phase transitions the surface transforms only partially into the non-nominal phase (see Fig. 1 in Ref. [19]).

[1] F. Fabre *et al.*, J. Phys. (Paris) **48**, 1017 (1987).
[2] E. D. Williams and N. C. Bartelt, Science **251**, 393 (1991).
[3] R. M. Tromp and M. C. Reuter, Phys. Rev. Lett. **68**, 820 (1992).
[4] J. Frohn *et al.*, Phys. Rev. Lett. **67**, 3543 (1991).
[5] C. Herring, Phys. Rev. **82**, 87 (1951).
[6] E. Conrad, Prog. Surf. Sci. **39**, 65 (1992), and references therein.
[7] H. M. van Pinxteren and J. W. M. Frenken, Europhys. Lett. **21**, 43 (1993); G. Bilalbegovic, F. Ercolessi, and E. Tosatti, Europhys. Lett. **17**, 333 (1992).
[8] G. M. Watson *et al.*, Phys. Rev. Lett. **71**, 3166 (1993).
[9] M. Flytzani-Stephanopoulos and L. D. Schmidt, Prog. Surf. Phys. **9**, 83 (1979). Surf. Sci. **272**, 118 (1992).
[10] G. Comsa, G. Mechtersheimer, and B. Poelsema, Surf. Sci. **97**, L297 (1980).
[11] G. Comsa, G. Mechtersheimer, and B. Poelsema, Surf. Sci. **119**, 159 (1982).
[12] E. Hahn, A. Fricke, and K. Kern, Surf. Sci. **297**, 19 (1993).
[13] Th. Michely and G. Comsa, Surf. Sci. **256**, 217 (1991).
[14] K. Kuhnke *et al.*, Surf. Sci. **272**, 118 (1992).
[15] N. C. Bartelt, T. L. Einstein, and E. D. Williams, Surf. Sci. Lett. **240**, L591 (1990).
[16] E. D. Williams *et al.*, Surf. Sci. **294**, 219 (1993).
[17] S. J. Sibener (private communication).
[18] R. J. Needs, M. J. Godfrey, and M. Mansfield, Surf. Sci. **242**, 215 (1991).
[19] M. Bott *et al.*, Phys. Rev. Lett. **70**, 1489 (1993).
[20] A. R. Sandy *et al.*, Phys. Rev. Lett. **68**, 2192 (1992).